Environmental Modeling of Silicon Dangling Bond QCA Wires

Dan Brox, Post-Doctorate research completed in the Department of Electrical and Computer Engineering, University of British Columbia, Vancouver, BC, Canada.

arXiv:1801.10221v1 [physics.app-ph] 24 Jan 2018

***Abstract*—Interactions of quantum cellular automata (QCA) circuits with their environment induce transitions in their quantum states that can cause errors in computation. The nature of these interactions depend on the specific physical implementation of the circuit. In the case of silicon dangling bond QCA, one channel of environmental interaction is between dangling bond cells and longitudinal phonons in the silicon lattice. In the presence of this environmental interaction, short 4 cell wire simulations show reliable operation at liquid nitrogen temperature, however simulation and theoretical arguments suggest long wires operated from thermal equilibrium are susceptible to exponential decay of cell polarization along their length regardless of clock zoning. Quantum annealing is suggested as a technique for bringing QCA wires into their ground state prior to information transmission to circumvent this problem.**

***Index Terms*—quantum, cellular automata, dangling bond, phonon**

I. Introduction

Computing schemes based on electronic quantum cellular automata (QCA) have been proposed as a route to performing classical computation higher speeds and lower power consumption than achievable with transistor-based architectures [1]. These schemes encode classical information via the electronic states of atomic-scale "cells" for which various physical implementations have been suggested [2-4]. QCA cells typically interact with each other electrostatically to alter each other's states, and so by carefully arranging cells in networks that constrain these interactions, circuits are created that digitally process the states of input cells to produce states of output cells, thereby performing computation.

An important feature of QCA computations is that it is desirable to maintain QCA circuits in their ground state throughout computation so that the final states of output cells are correctly determined by the states of input cells. A process of gradually modulating the tunneling barriers of cells while input cell polarizations are switched has been proposed as a means of maintaining the ground state. In this process, known as adiabatic switching [1], a circuit beginning in its ground state is guaranteed to be found in its ground state at the end of computation with high probability if switching occurs slowly enough, according to the adiabatic theorem of quantum mechanics [5].

One difficulty with the adiabatic clocking scheme is that although it can maintain a closed QCA circuit in its ground state, the adiabatic theorem does not account for interactions of the circuit with its environment that may cause transitions to excited states. This problem persists even when a circuit is held in a static configuration in which equilibrium thermal effects are easily computed. For instance, consider a QCA wire with Hamiltonian:

$$H_{wire} = -P_{in}\frac{E_k}{2}\sigma_z^1 - \frac{E_k}{2}\sum_{i=1}^{N-1}\sigma_z^i\sigma_z^{i+1}, \tag{1}$$

where each cell i is in a $|0\rangle$ or $|1\rangle$ σ_z^i eigenstate, E_k is the energetic cost of having adjacent cells in different states, and P_{in} is the input polarization that affects the state of cell 1 and thereby influences the states of all cells along the wire. If we assume that the input polarization is $+1$, the ground state of the wire is $|1,1,1,....1,1\rangle$ (N 1's). In contrast, excited states of the wire contain a nonzero number of kinks, and we can expect that the last cell of the wire is in the $|0\rangle$ or $|1\rangle$ state depending on whether the total number of kinks is odd or even. If the wire is in thermal equilibrium with its surroundings at temperature T, then the Boltzmann factor associated with a kink of energy E_k is $p = e^{-\frac{E_k}{k_B T}}$, and the probabilities of the M^{th} cell in the wire occupying the $|0\rangle$ or $|1\rangle$ are calculated to be:

$$Prob(|0\rangle) = \frac{(1+p)^M - (1-p)^M}{2(1+p)^M}, \tag{2}$$

$$Prob(|1\rangle) = \frac{(1+p)^M + (1-p)^M}{2(1+p)^M}. \tag{3}$$

This means that the expected polarization of the M^{th} (output) cell is:

$$\frac{Prob(|1\rangle) - Prob(|0\rangle)}{Prob(|1\rangle) + Prob(|0\rangle)} = \frac{(1-p)^M}{(1+p)^M}, \tag{4}$$

which decays to 0 as $M \to \infty$. This indicates that for sufficiently long wires, in the absence of clocking (i.e. time independent Hamiltonian), thermal effects can completely destroy the information we expect to see propagated by the wire.

This same thermal issue also poses problems for any sufficiently large QCA circuit in a static state, so it is interesting to ask if the dynamics of QCA computation can be employed to prevent thermal degradation. To this end, it has been suggested that if a QCA circuit is divided into sufficiently small individually clocked subcircuits or "zones", then each subcircuit can perform computation with high fidelity so that appropriate circuit architecture can be used to solve the problem [1]. However, it is not clear that this zoning hypothesis is true,

and little simulation work has been done to verify this is true for specific circuit-environment interactions and zoning schemes. Furthermore, better understanding of this issue is critical to deciding how large QCA circuits can be made before other classical computing elements must be included into their architecture [6] to make useful devices. Therefore, in this paper we investigate the effect of zoning and electron-phonon interactions on a silicon dangling bond QCA wire to ascertain how effective zoning is in preventing thermal degradation in this particular case.

II. QCA Wire Zoning

To introduce the notion, we consider a simple silicon dangling bond QCA circuit which we'll take to be a straight wire. Each cell in this wire consists of two silicon dangling bonds and a single electron which is localized at either site during latching and shared between sites during cell relaxation. A schematic of an 8 cell wire partitioned into four zones in shown in Fig. 1.

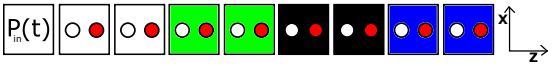


Fig. 1 Schematic of an 8 cell silicon dangling bond QCA wire partitioned into four zones.

Since we are interested in adiabatically clocking the cells to transmit information along the wire, the relevant time dependent Hamiltonian for the wire is:

$$H_{wire}(t) = -P_{in}(t)\frac{E_k}{2}\sigma_z^1 + \frac{E_k}{2}\sum_{i=1}^{N}\gamma^i(t)\sigma_x^i - \frac{E_k}{2}\sum_{i=1}^{N-1}\sigma_z^i\sigma_z^{i+1}, \quad (5)$$

where the input polarization is now time dependent and tunneling modulators $\gamma^i(t)$ are employed to latch and delatch the states of the cells. For specificity, we choose a kink energy of $E_k = 0.05$ eV and maximum tunneling modulation $max|\gamma^i(t)| = 1.0$. These values are representative of a QCA wire composed of silicon dangling bond qubits [4]. It is important to note that the adiabatic clocking assumed in equation (5) has not been physically implemented in any silicon dangling bond circuit to date, and technical challenges to modulating the intercell tunneling as necessary are presented by the atomic dimensions of the cells. Nevertheless, silicon dangling bond technology is still in early stages of development, so a standard form of the QCA wire Hamiltonian has been adopted here for ease of comparison with other theoretical work and to suggest specifications on the modulation in anticipation of a technique for physically implementing it.

Simulation of different zoning schemes are made by choosing different input polarization functions and tunneling modulation functions. For instance, the Fig. 2 shows an 8 cell wire divided into 4 clocking zones, and four (normalized) clocking signals Clock 1 ($\gamma^1(t) = \gamma^2(t)$), Clock 2 ($\gamma^3(t) = \gamma^4(t)$), Clock 3 ($\gamma^5(t) = \gamma^6(t)$), and Clock 4 ($\gamma^7(t) = \gamma^8(t)$).

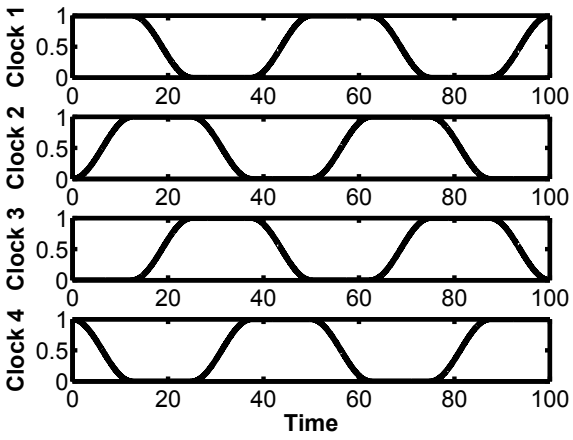


Fig. 2 Four phase clocking of a QCA wire.

The clocking signals are shown over 2 complete periods in time units of $\hbar/E_k$. When a clock signal is low, the corresponding cell is latched in a fixed σ_z eigenstate, and when it is high the corresponding cell is in a relaxed unlatched state where it can be influenced by the state of its neighbors. This is the reason for applying 4 clock phases in succession to iteratively latch and unlatch data along the wire and pipeline information flow.

For the purposes of investigating the interplay between wire zoning and phonon interaction, we can consider simple information transmission processes in which the input polarization is fixed at 1 throughout. To do this, we begin with the each wire cell in its relaxed state $\gamma^i(0) = \gamma_{max}$, and switch the cells from their relaxed state to hold states in various ways, examining the expected polarization of each of the cells throughout. For instance, in the case of a four cell wire, we could use 1 clocking zone and clock all the cells to the hold state simultaneously, or use 2 clocking zones to clock cells 1 and 2 to a hold state and lag the clocking of cells 3 and 4 to the hold state by a quarter phase as in the 4 phase clocking scheme. We could also use 4 zones, separately clocking each of the zones with a quarter lag phase between the switching to the hold state of each. This clocking scheme is illustrated in Fig. 3. Note that in this particular scheme, once a particular zone is latched, it remains latched for the rest of the process.

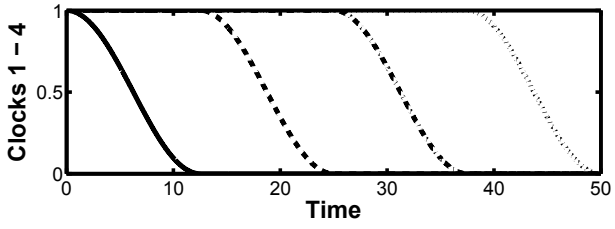


Fig. 3 Sequential latching of a QCA wire divided into 4 clocking zones.

Regardless of the clocking scheme employed, the $t = 0$ initial state of the wire for each process is the same, and in this state the expected polarization of the cells approaches 0 as we move further from the driver cell as indicated in Table 1.

TABLE I: Initial polarizations of cells in a relaxed four cell wire with input polarization 1.

	Cell 1	Cell 2	Cell 3	Cell 4
Initial Polarization	0.8276	0.7221	0.6078	0.4472

Therefore, it is necessary to latch the cells of the wire into hold states so that their polarizations are able to follow the input polarization and convey information along the wire.

III. Phonon Interaction

To better understand environmental effects on silicon dangling bond QCA circuits, we must first specify a particular interaction, which we take here to be the interaction between the cells fabricated on a silicon crystal surface and phonons propagating through the silicon lattice. For simplicity, we'll only consider the primary influence of longitudinal phonons in the silicon lattice on the dangling bond QCA wire. Unlike transversely polarized phonons, longitudinal phonons generate charge density variations by compressing and stretching the lattice in their direction of motion, thereby interacting electrostatically with electrons.

To model this, we first write the Hamiltonian of the QCA wire interacting with the longitudinal phonons in the silicon lattice [7]:

$$H_{total} = H_{wire} + H_{int} + H_{ph}, \tag{6}$$

where:

$$\begin{aligned} H_{wire}(t) &= -P_{in}(t)\frac{E_k}{2}\sigma_z^1 + \frac{E_k}{2}\sum_{i=1}^{N}\gamma^i(t)\sigma_x^i \\ &\quad -\frac{E_k}{2}\sum_{i=1}^{N-1}\sigma_z^i\sigma_z^{i+1}, \end{aligned} \tag{7}$$

$$H_{ph} = \sum_{\vec{q}}\hbar\omega_q\left(a_{\vec{q}}^{\dagger}a_{\vec{q}} + \frac{1}{2}\right), \tag{8}$$

and the energy of interaction with electrons, known as the deformation potential energy, is given by (c.c denotes complex conjugate):

$$\begin{aligned} H_{int} &= \int d^3r Z_{DP}\psi^{\dagger}(r)\psi(r) \\ &\quad \cdot\left(\sum_{\vec{q}} iq\sqrt{\frac{\hbar}{2\Omega V\omega_q}}a_{\vec{q}}e^{i\vec{q}\cdot r} + c.c.\right). \end{aligned} \tag{9}$$

In these equations, $\vec{q}$ indexes all possible wave vectors of the longitudinal phonon modes, $a_{\vec{q}}^{\dagger}$ and $a_{\vec{q}}$ are the creation and annihilation operators of a phonon in a particular mode, $\hbar\omega_q$ is the energy of the phonon mode $\vec{q}$ dependent on the wave vector length $q = \parallel \overrightarrow{q} \parallel$, $Z_{DP} \approx 3.3$ eV is the deformation potential in silicon, Ω is the density of silicon, V is the total volume, and:

$$\psi(r) = \sum_{i,\sigma}\phi_{i\sigma}(r)c_{i\sigma}, \tag{10}$$

$$\psi^{\dagger}(r) = \sum_{i,\sigma}\phi_{i\sigma}^{*}(r)c_{i\sigma}^{\dagger}, \tag{11}$$

$$[c_{i\sigma}, c_{j\sigma}^{\dagger}] = \delta_{ij}, \tag{12}$$

are fields that create and annihilate electons at point **r**. The indices (i,σ) index single electron states localized at QCA cell i with symmetry σ. $\phi_{i\sigma}(r)$ is the wave function corresponding to this electron. The operator $n(r) = \psi^{\dagger}(r)\psi(r)$ is the local electron density at point **r**.

The next task is to use the Hamiltonian for the QCA wire-phonon system to derive an approximate equation for the quantum evolution of the QCA wire alone. In so doing, we must appreciate that the quantum state of the wire is entangled with the phonon state of its environment, and so if we wish to describe its quantum state independently of the environment we should do so with a density matrix. More precisely, we should describe the state of the entire QCA wire-phonon system with a density matrix ρ_{system} whose evolution is described by the Von Neumann equation:

$$\frac{d}{dt}\rho_{system} = -\frac{i}{\hbar}[H_{total}, \rho_{system}], \tag{13}$$

and use some procedure of averaging over environmental effects to obtain an approximate equation of evolution for the density matrix of the wire ρ_{wire} alone. For our purposes, we take this approximate equation to be a Lindblad master equation for the density matrix of the QCA wire [8]:

$$\begin{aligned} \frac{d}{dt}\rho_{wire} &= -\frac{i}{\hbar}[H_{wire}, \rho_{wire}] \\ &\quad +\sum_{r,s}\frac{1}{2}W_{rs}\left(2P_{rs}\rho_{wire}P_{sr} - [P_{sr}P_{rs}, \rho_{wire}]\right), \end{aligned} \tag{14}$$

where r and s index different (instantaneous) eigenstates of the QCA wire, P_{rs} is the state transition operator:

$$P_{rs} = |r\rangle\langle s|, \tag{15}$$

and the constants W_{rs} are the environmentally induced transition rates from state $|s\rangle$ to $|r\rangle$ [9-10]:

$$\begin{aligned} W_{rs} &= \sum_{\vec{q}}\frac{\pi Z_{DP}^2 q^2}{\Omega V\omega_q}|\langle r|\beta(\vec{q})|s\rangle|^2 n_{ph}\left(E_q, T\right) \\ &\quad \cdot\delta\left(E_q - (E_r - E_s)\right),\ E_r > E_s, \end{aligned} \tag{16}$$

$$\begin{aligned} W_{rs} &= \sum_{\vec{q}}\frac{\pi Z_{DP}^2 q^2}{\Omega V\omega_q}|\langle r|\beta^{\dagger}(\vec{q})|s\rangle|^2 \\ &\quad \cdot\left(n_{ph}\left(E_q, T\right) + 1\right)\delta\left(E_q - (E_s - E_r)\right),\ E_r < E_s. \end{aligned} \tag{17}$$

In these formulae, Z_{DP} is the deformation potential energy (3.3 eV in silicon), Ω is the density of silicon 2.33×10^3 kg·m^{-3}, V is the total volume of silicon, T is the temperature, $c_s = 9.0 \times 10^3$ m·s^{-1} is the speed of sound in silicon, and $E_q = \hbar\omega_q = \hbar c_s q$ is the energy difference between wire states $|s\rangle$

and $|r\rangle$. The phonon thermal occupation number $n_{ph}\left(E_q, T\right)$ is:

$$n_{ph}\left(E_q, T\right) = \left(e^{\hbar c_s q/k_B T} - 1\right)^{-1}, \tag{18}$$

and the QCA cell transition operator $\beta(\vec{q})$ is defined as:

$$\beta(\vec{q}) = \sum_i \sigma_z^i \langle S_i | e^{i\vec{q}\cdot r} | A_i \rangle + \sigma_x^i \langle L_i | e^{i\vec{q}\cdot r} | R_i \rangle, \tag{19}$$

where the matrix elements are between different electronic states of the QCA cells defined as:

$$|L_i\rangle \leftrightarrow \frac{1}{\sqrt{\pi a_B^3}} e^{-r_{Li}/a_B},\ r_{Li} = \left\| \vec{r}_i + \frac{1}{2} D \overrightarrow{k} \right\|, \tag{20}$$

$$|R_i\rangle \longleftrightarrow \frac{1}{\sqrt{\pi a_B^3}} e^{-r_{Ri}/a_B},\ r_{Ri} = \left\| \vec{r}_i - \frac{1}{2} D \overrightarrow{k} \right\|, \tag{21}$$

$$|S_i\rangle = \frac{1}{\sqrt{2}} \left(|L_i\rangle + |R_i\rangle \right), \tag{22}$$

$$|A_i\rangle = \frac{1}{\sqrt{2}} \left(|L_i\rangle - |R_i\rangle \right). \tag{23}$$

In these equations,$\vec{k}$ is the unit vector in z direction, L is the distance between cells in the wire, and $r_i = iL\vec{k}$ is the position of the i^{th} cell.

As an example, we can compute the transition rates for a single cell wire at $T = 300$ K. For a single cell, the kink energy and its dependence on L does not factor into the system Hamiltonian, so it suffices to adopt an intercell atomic distance and tunneling (i.e. relaxation) energy to determine the rates. Therefore, choosing $D = 7.68 \times 10^{-10}$ m and a tunneling energy of 0.05 eV, we obtain:

$$W_{10} = 3.60 \times 10^{12}\, s^{-1}, \tag{24}$$

$$W_{01} = 2.46 \times 10^{13}\, s^{-1}. \tag{25}$$

In the requisite calculations, a renormalized Bohr radius of $a_B = 2.79 \times 10^{-10}$ m is used to ensure the value of the expected tunneling determined by the electron wave functions is in fact 0.05 eV. In more general calculations, the Bohr radii a_B of each cell is similarly renormalized at each time step according to the tunnelings $\gamma^i(t)$, influencing the β operators and induced transition rates betwen wire states W_{rs} and W_{sr}. Note that the β operator can be thought of as a perturbation of H_{total} induced by stretching and compressing of the silicon lattice, and this is appropriately thought of as a modulation of intercell tunneling, not intracell electrostatic coupling [11]. For this reason, although we consider 2-atom QCA cells here for simplicity, we can expect phonon induced transitions to have an effect of similar magnitude on more standard 4-atom QCA cells. Also note that for sufficiently long wires, the Born approximation used in deriving the Lindblad master equation is no longer valid (see Appendix A), and in such cases the Lindblad equation must be regarded as a hypothetical model of the system-environment interaction rather than a rigorous approximation of the true system evolution.

IV. Zoning and Transition Rates

We can now examine the effect of phonon interaction on the expected polarization wire cells at the end of latching. To do this we need to assert the initial state of the wire, which we take to be the ground state of a four cell wire with fixed input polarization 1 and all cells relaxed. As an initial study, we only enable transitions between the ground and first four excited states of the wire (W_{sr}, $W_{rs} = 0$ unless $r = 0$ and $s \in \{1, 2, 3, 4\}$), and perform switching at $T = 300$ K, $k_B T = 0.026$ eV over a total adiabatic clocking time of $20\hbar/E_k = 1.31 \cdot 10^{-12}$ s^{-1}. This does not take into account the full complexity of the environmental interaction bringing the wire to a state of thermal equilibrium, but does account for the primary excitation channels of the ground state into excited states. Note that the reverse excited-to-ground state transition rates are related to the ground-to-excited state rates by Boltzmann factors:

$$W_{rs} = W_{sr} \cdot e^{(E_s - E_r)/k_B T}, \tag{26}$$

to ensure detailed balance between the state populations at thermal equilibrium.

Under our assumptions, we can use the Lindblad equation to compute and plot the cell output polarizations at the end of each clocking process shown in Fig. 4.

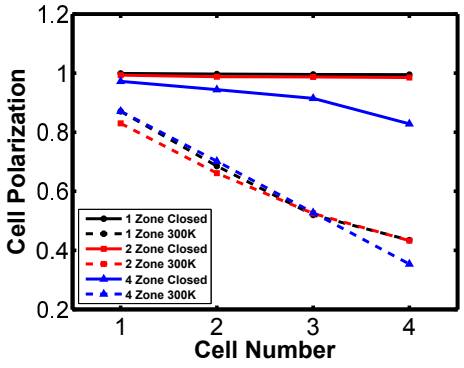


Fig. 4 Cell polarizations of four cell wire at the completion of different clocking processes run at T=300 K.

In Fig. 4, the closed system polarizations are close to 1, and the 4 zone closed system polarizations can be increased to the level of the 1 and 2 zone closed system polarizations by doubling the adiabatic switching time to $40\hbar/E_k$. Note that at $T = 300$ K, the polarizations of Cell 4 at the end of each process are significantly lower than the closed system polarizations, indicating that the phonon interaction has degraded reliability of information transmission. This is because the kink energy $E_k = 0.05$ eV for silicon dangling bond circuits is close to the room temperature thermal energy $k_B T = 0.026$ eV, so the total induced transition rate

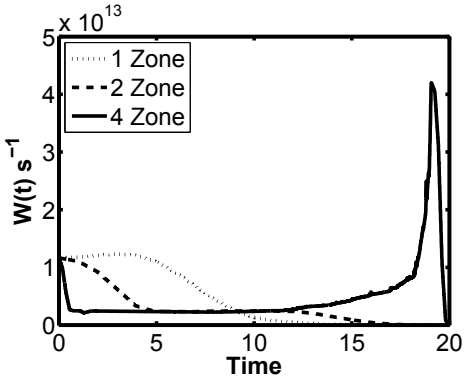


Fig. 5 Ground to first excited state transition rates as a function of time throughout the duration of different clocking processes.

$W = W_{10} + W_{20} + W_{30} + W_{40}$ for each zoning is large enough to have a significant effect over the process duration. Specifically, the rates for each zoning are plotted in Fig. 5, indicating $max\, W > 10^{13}$ s^{-1}in each case, from which it follows that the timescale for excitation out of the ground state $1/W < 10^{-13}$ s is short compared with the total adiabatic switching time to the duration of adiabatic switching. In this regime, the Born approximation does not hold, so the Lindblad equation is not strictly accurate, but the results suggest the operating temperature may have to be lowered below room temperature for short silicon dangling bond wires to function effectively.

Lowering to liquid nitrogen temperature (77 K), the new expected output cell polarizations after each process has been completed are shown in Fig. 6.

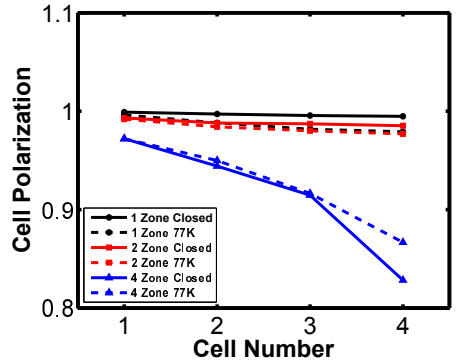


Fig. 6 Cell polarizations of four cell wire at the completion of different clocking processes run at $T = 300$ K.

The plots show that lowering the temperature has succeeded in restoring wire performance to its closed system performance by lowering the ground-to-excited state transition rates. Note that the excited-to-ground state transition rates are still large, and this is why the 4 zone cell 4 polarization actually increases when environmental interactions are taken into account instead of decreasing like in the other cases. Changing wire length, temperature, and QCA parameters, it is not strictly true that using more zones protects wire performance better against phonon interaction. However, when this is the case, it is typically because many of the transition rates W_{rs} vanish during portions of the adiabatic switching cycle when multiple clocking zones are used due to additional symmetry of the time dependent Hamiltonian that occurs once a particular cell is latched. Specifically, from the form of the wire Hamiltonian:

$$H_{wire}(t) = -P_{in}(t)\frac{E_k}{2}\sigma_z^1 + \frac{E_k}{2}\sum_{i=1}^{N}\gamma^i(t)\sigma_x^i - \frac{E_k}{2}\sum_{i=1}^{N-1}\sigma_z^i\sigma_z^{i+1}, \quad (27)$$

it follows that if $\gamma^i(t) = 0$, then σ_z^i commutes with $H_{wire}(t)$:

$$[\sigma_z^i, H_{wire}(t)] = 0. \quad (28)$$

This means the Hamiltonian and i^{th} spin can be simultaneously diagonalized, or equivalently, that the energy eigenstates of $H_{wire}(t)$ may be split into two groups depending on the eigenvalue of σ_z. In turn, this implies that if $|s_{+1}\rangle$ and $|s_{-1}\rangle$ are any two eigenstates of the Hamiltonian with different i^{th} cell spin eigenvalues:

$$\sigma_z^i|s_{+1}\rangle = |s_{+1}\rangle, \quad (29)$$

$$\sigma_z^i|s_{-1}\rangle = -|s_{-1}\rangle, \quad (30)$$

then the induced phonon transitions between these states is zero:

$$\langle s_{-1}|\sigma_z^i|s_{+1}\rangle = 0. \quad (31)$$

Furthermore, for any other operator S that commutes with σ_z^i:

$$[\sigma_z^i, S] = 0, \quad (32)$$

we have:

$$\langle s_{-1}|[\sigma_z^i, S]|s_{+1}\rangle = 0, \quad (33)$$

$$\Rightarrow \langle s_{-1}|\sigma_z^i S - S\sigma_z^i|s_{+1}\rangle = 0, \quad (34)$$

$$\Rightarrow \langle s_{-1}| - S - S|s_{+1}\rangle = 0, \quad (35)$$

$$\Rightarrow \langle s_{-1}|S|s_{+1}\rangle = 0. \quad (36)$$

Noting that $[\sigma_z^i, \sigma_z^j] = [\sigma_x^i, \sigma_x^j] = 0$ for all cell indices i and j, and that $[\sigma_x^i, \sigma_z^j] = 0$ for all indices $i \neq j$, it follows the operator $\beta(\vec{q})$ (equation (19)) which is a linear sum of these operators and responsible for environementaly induced transitions (equations (16) and (17)) does not induce transitions between several pairs of states once multiple cells are latched. In many cases this enhanced symmetry results in improved wire performance in the presence of phonon interactions.

V. Gain and Dissipation

The results of the previous section showed that if a short 4 cell silicon dangling bond wire begins in its ground state, then room temperature phonon interactions induce transitions in the wire at rates that make information transmission unreliable. However, lowering to liquid nitrogen temperature restored successful information transmission by increasing the timescale for excitation out of the ground state to a value greater than the adiabatic switching interval. Determination of whether or not reliable information transmission over long silicon dangling bond wires initialized in their ground state is achievable at low temperature requires different modeling techniques, since the Born approximation of weak environmental interaction required to validate use of the Lindblad equation no longer holds for sufficiently large numbers of cells (see Appendix A).

Another issue is that even if we ignore environmentally induced transitions that may occur during information transmission, thermal degradation can also occur due to thermalization of the initial wire state. That is, if the wire has been unused for a sufficiently long duration, we expect it reside in a mixed state of thermal equilibrium rather than its ground state. To investigate this, we neglect all induced transitions ($W_{rs} = 0$) and consider closed system processes beginning from a state of thermal equilibrium. Fig. 7 shows the results of simulating an information transmission process along an 8 cell wire with fixed input polarization and all cells relaxed, starting from the ground state ($T = 0$ K). It plots the output polarizations of each of the wire cells after 4 processes with different zonings are completed. The total duration of each process is $40\hbar/E_k$.

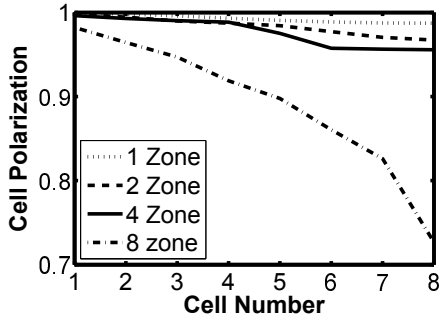


Fig. 7 Output cell polarizations of an eight cell wire after different clocking processes beginning from thermal equilibrium.

The plot shows that when the wire is closed and 1,2, or 4 zones are used, the switching time is sufficiently long for high fidelity information transmission. When 8 zones are used, the switching of individual cells is faster and non-adiabatic transitions to excited states occur and signifcantly increase the probability of error [12].

Fig. 8 shows two plots of the same information transmission process beginning from thermal equilibrium states at $T = 77$ K and $T = 300$ K, respectively. These plots indicate that regardless of the zoning scheme, beginning transmission from a thermal state results in polarization decay of the cells along the wire. The exponential nature of the decay in polarization as described in Section I is clearly evident at $T = 300$ K where thermal errors dominate any transmission errors due to non-adiabatic transitions when 8 clocking zones are used.

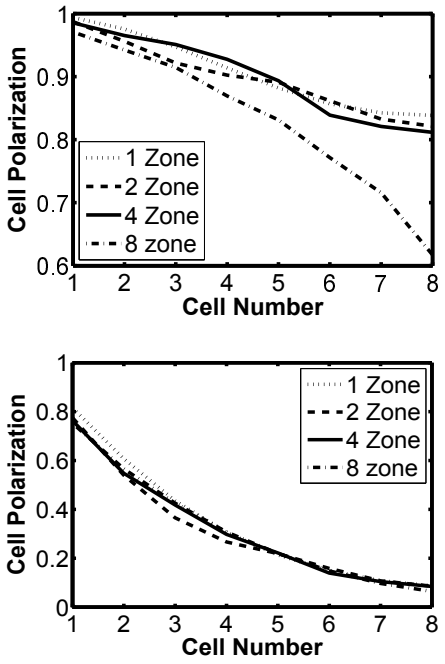


Fig. 8 Output cell polarizations along an 8 cell wire beginning information transmission from thermal equilibrium at $T = 77$ K (top) and $T = 300$ K (bottom).

We can also examine a different process with fixed input polarization 1 which begins from a thermal equilibrium state at $T = 300$ K in which all the cells are latched (clock signals are zero). In this initial state, the cell polarizations decay exponentially along the wire away from the input as in the introductory example of Section I. From this state, each cell in the wire is relaxed and relatched sequentially to transmit the input polarization along the wire. Fig. 9 shows the cell polarizations before and after the process. Once again, the cell polarizations decay along the wire exponentially after switching is finished.

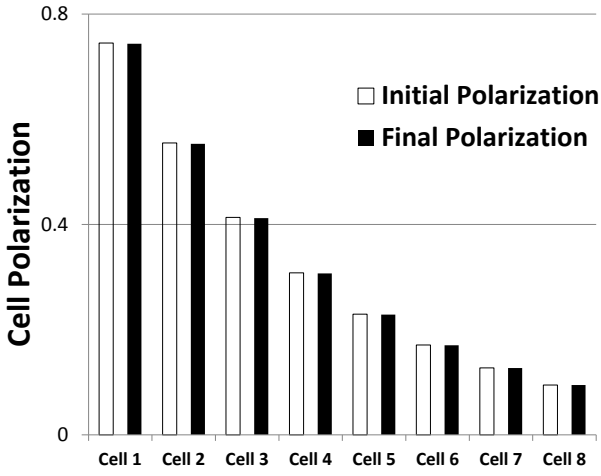


Fig. 9 Cell polarizations before and after a switching process run from a latched thermal equilibrium state.

These results show that even at liquid nitrogen temperature, operating a relatively short silicon dangling bond wire from thermal equilibrium will result in exponential decay of polarization and limit its ability to transmit information. Furthermore, the results hold true regardless of the zoning scheme, so in this circumstance polarization amplification is absent. That is, the expected output polarization of a zone is not amplified, as measured by the expected polarization of the next zone, so there is no gain in the polarization as we might hope for. However, this is what we should expect for an adiabatic process which evolves excited states into other excited states, since this implies a thermally mixed state will evolve under coherent evolution into a different mixture of excited states. It follows that if we are to obtain the correct output polarization across a QCA wire operated from thermal equilibrium, it must be a consequence of dissipative environmental effects which can induce transitions from excited to lower energy wire states during adiabatic switching. One possibility is that induced transitions occur in such a manner that individual zones are brought to thermal equilibrium quickly relative to their adiabatic switching time. In this event, if the zones are sufficiently small, each zone will be brought into its ground state with its cells following the input polarizations with high probability.

To investigate this possibility, for simplicity, we can assume that zones consist of single cells. In this event, assuming a particular cell in the wire experiences an input polarization $P \in [0,1]$, then:

$$P = q(1) + (1-q)(-1) = 2q - 1, \tag{37}$$

where q is the probability that the input cell brought to thermal equilibrium has polarization $+1$. Letting $p = e^{-E_k/k_BT}$, it follows that the expected cell output polarization after thermal equilibrium is reached is:

$$Pol = \frac{q + (1-q)p - (1-q) - qp}{q + (1-q)p + (1-q) + qp} = (2q-1)\frac{1-p}{1+p}, \tag{38}$$

which is smaller than the input polarization by a factor of $(1-p)/(1+p)$. This implies polarization decay also occurs in this situation. This is an important point, since in a model of the cell where the input polarization is regarded as a continous function [13] rather than a cell with discrete polarizations we would have:

$$Pol = \frac{1 - e^{-P\cdot E_k/k_BT}}{1 + e^{-P\cdot E_k/k_BT}}, \tag{39}$$

instead, and this model does exhibit polarization gain for small input polarizations P whenever $\frac{E_k}{k_BT} > 2$:

$$Pol = \frac{1 - e^{-P\cdot E_k/k_BT}}{1 + e^{-P\cdot E_k/k_BT}} > P, \tag{40}$$

It is easy to verify that the former polarization decay formula holds instead of the polarization gain formula for a 2 cell wire latching process with each cell clocked individually. Assuming a kink energy of 0.05 eV and operating temperature satisfying $k_BT = 0.017$ eV, we can use the Lindblad equation with transition rates:

$$W_{rs} = C \cdot |\langle\psi_r|\sigma_x^1|\psi_s\rangle|^2, \tag{41}$$
$$W_{sr} = e^{(E_s - E_r)/k_BT} W_{rs}, \tag{42}$$

while the first cell is latched, and transition rates:

$$W_{rs} = C \cdot |\langle\psi_r|\sigma_x^2|\psi_s\rangle|^2, \tag{43}$$
$$W_{sr} = e^{(E_s - E_r)/k_BT} W_{rs}, \tag{44}$$

while the second cell is latched. These transitions act to flip the z-polarization of the first or second cell respectively, and choosing the constant C sufficiently large brings the first and second cells into thermal equilibrium during their respective latchings. At the end of this process, the simulation gives cell polarizations:

$$Cell\,1\,Pol = 0.8997 = \frac{1-p}{1+p}, \tag{45}$$
$$Cell\,2\,Pol = 0.8095 = \left(\frac{1-p}{1+p}\right)^2. \tag{46}$$

Note that the second polarization is not:

$$\frac{1 - e^{-0.8997\cdot E_k/k_BT}}{1 + e^{-0.8997\cdot E_k/k_BT}} = 0.8675, \tag{47}$$

as would be the case if the formula exhibiting polarization gain held true.

VI. Quantum Annealing

Given that operating a QCA wire from thermal equilibrium results in exponential polarization decay in both cases of purely coherent evolution and strong decoherence, the question arises as to whether or not there are any other techniques for bringing wires into their ground state with high probability either before or during information transmission. One way of doing this is to adiabatically switch the wire through a state where at thermal equilibrium it occupies its ground state with very high probability. For instance, in the event that the tunneling coefficients γ^i can be raised to very large ($\gg E_k$) values, the wire cells may effectively decouple, and the entire wire will reach thermal equilibrium as each of its cells reaches its own state of thermal equilibrium. Therefore, adiabatically switching the wire through this high tunneling regime might be used as a means of restoring the wire ground state with high probability at regular intervals to avoid occupying information scrambling thermal states. This process is known as quantum annealing [14].

For large γ^i, each cell will occupy its ground state with high probability once it has equilibrated, since at equilibrium this probability is:

$$p_{gnd} = \frac{1}{1 + e^{-\gamma_{max}/k_BT}}. \tag{48}$$

It follows that the probability of an N cell wire occupying its ground state is p_{gnd}^N. For 1000 completely decoupled silicon dangling bond cells operating at liquid nitrogen temperature and maximum tunneling $\gamma_{max} = 0.05$ eV, the probability

of the array occupying its ground state after relaxation is 0.32, but increases to 0.9993 when $\gamma_{max} = 0.1$ eV. In practice, larger maximum tunnelings may be required due to the z-polarization coupling terms in the QCA Hamiltonian. If tunneling modulation can be implemented in silicon dangling bond technology, it is possible such maximum tunnelings are achievable, although a mechanism other than phonon emission/absorption will be necessary to relax cells since the longitudinal acoustic phonon spectrum only extends up to 0.063 eV. Therefore, utilizing this strategy for silicon dangling bond QCA requires further progress in engineering dangling bond cells with large and tuneable tunneling and identifying environmental interactions that can relax cells on a suitable timescale.

VII. Conclusions

Simulations of 4 cell silicon dangling bond wires suggest they can operate reliably from their ground state at liquid nitrogen temperature due to reduced environmentally induced excitations of the ground state. However, simulations of longer wires initialized in states of thermal equilibrium show exponential decay of cell polarization along the wire regardless of clock zoning. Further theoretical arguments and simulation suggest this polarization decay persists even when environmental transitions bring wire zones to local thermal equilibrium quickly. To solve this problem, a quantum annealing process whereby cell tunnelings are ramped to a level significantly greater than the intracell coupling is proposed as a method of periodically re-initializing the wire in its ground state with high probability. In principle, the same technique could be used to bring arbirary QCA circuits into their ground state, although for realization this approach requires engineering cells with large and tunable maximum tunneling, which is an ongoing topic of research in the development of silicon dangling bond technology.

Acknowlegment

This post-doctorate work at the University of British Columbia was supported by an NSERC Engage grant in parternship with Quantum Silicon Inc.

Appendix A: Validity of Master Equation

The Lindblad equation introduced in Ssection 3:

$$\begin{aligned}\frac{d}{dt}\rho_{wire} &= -\frac{i}{\hbar}[H_{wire},\rho_{wire}] \\ &\quad + \sum_{r,s}\frac{1}{2}W_{rs}\left(2P_{rs}\rho_{wire}P_{sr} - [P_{sr}P_{rs},\rho_{wire}]\right),\end{aligned} \tag{49}$$

is used to describe the interaction of a QCA wire with phonons in its environment. The derivation of this equation from the coherent quantum dynamics of the wire and phonon bath taken together relies on using the Born, Markov, and secular approximations in succession. Together, the correctness of the Born and Markov approximations imply the applicability of the Bloch-Redfield master equation. The secular approximation is then used to neglect particular terms in the Bloch-Redfield master equation, giving rise to the Lindblad master equation. These approximations are detailed below:

1) Born approximation: The effect of the interaction of the phonon bath with the QCA wire is weak, and may be treated as a perturbation of the coherent wire dynamics. This implies the sum of the induced transition rates W_{rs} into or out of any state is small compared to the characteristic energy scale of the system and adiabatic clocking frequency:
$$\sum_r W_{rs} \ll E_k/\hbar = 1.52\cdot 10^{13}s^{-1}. \tag{50}$$
2) Markov approximation: The fluctuations away from thermal equilibrium of the phonon bath occur on a timescale that is much shorter than the characteristic timescales of interaction of the phonon bath and QCA wire as determined by the phonon induced transition rates:
$$\sum_r W_{rs} \ll \omega_{q_{max}} = 1.06\times 10^{14}s^{-1}. \tag{51}$$
3) Secular approximation: All internal transition frequencies of the QCA wire $\omega_{ij} = \hbar E_{ij}$ are significantly larger than the phonon induced transition rates:
$$\sum_r W_{rs} \ll \hbar E_{ij}, \tag{52}$$
This condition implies various terms in the Bloch-Redfield master equation average to zero. This is a more stringent condition than the Born approximation, since any degeneracy of states in the QCA wire will prevent this condition from holding true.

Notably, the secular approximation does not generally hold for adiabatic clockings of QCA circuit with multiple cells because of degeneracies and near degeneracies of wire states. Because of this, when the Born and Markov approximations hold, it is more accurate to consider the QCA wire as satisfying a Bloch-Redfield master equation, which written in the interaction picture is [8]:

$$\dot{\rho}^{(i)}_{s's}(t) = \sum_{m,n}\gamma_{s'smn}(t)\rho^{(i)}_{mn}(t), \tag{53}$$

$$\begin{aligned}\gamma_{s'smn}(t) &= [-\sum_k \delta_{sn}\Gamma^+_{s'kkm} + \Gamma^+_{nss'm} \\ &\quad + \Gamma^-_{nss'm} - \sum_k \delta_{sn}\Gamma^+_{s'kkm}]e^{i(\omega_{s's}-\omega_{mn})}.\end{aligned} \tag{54}$$

In this equation, the $\Gamma^{\pm}$ terms are various relaxation rates between states expressible in terms of the system-bath interaction. The secular approximation assumes that only transition rates γ_{ssss}, γ_{ssmm} $(s \neq m)$, and $\gamma_{s'ss's}$ are nonzero. In this case:

$$\gamma_{ssmm}(t) = W_{sm}, \tag{55}$$

This rough approximation is assumed in Section 4 for four cell wires with only 16 total states, since the states for a single clocking zone are typically non-degenerate. Also, many of the transition rates that are ignored in making the secular

approximation vanish for much of adiabatic switching when multiple clocking zones and state degeneracies occur.

Having justified the use of the secular approximation for short wires, we can now go back and analyze when we expect the Born and Markov approximations to hold true, since we can expect that as a QCA circuit gets larger, phonon induced transition rates will in some sense begin to dominate its dynamics. Since the induced transition rates vary during adiabatic switching, we can, as a rough estimate, consider sums of induced rates $\sum W_{r0}$ at $T = 77$ K out of the ground state of N cell silicon dangling bond arrays with zero intercell coupling and input polarization, and tunneling energy $\gamma^i(t) = 0.05$ eV. In this example, a phonon can be absorbed by any cell to excite the wire ground state to the $N-$fold degenerate first excited state, and the sum of transition rates is empirically:

$$\sum W_{r0} \approx 1.2 \cdot 10^{10} N,$$

which is equal to the characteristic frequency $E_k/\hbar = 1.52 \cdot 10^{13}$ s^{-1} when $N = 1270$. Therefore, as an initial estimate we can guess the Born approximation begins to fail at $T = 77$ K for wires approximately 1000 cells in length.

VIII. References

[1] C. Lent, P. Tougdaw, "A device architecture for computing with quantum dots", *Proc. IEEE,* vol. 85, no. 4, pp. 541 - 557, 1997.

[2] C. Lent, P. Tougaw, "Bistable saturation due to single electron charging in rings of tunnel junctions", *Journal of Applied Phys*ics, vol. 75, no. 8, pp. 4077 - 4080, 1994.

[3] C. Lent, B. Isaksen, and M. Lieberman, "Molecular quantum-dot cellular automata", *Journal of the American Chemical Society,* vol. 125, no. 4, pp. 1056 - 1063, 2003.

[4] L. Livadaru, P. Xue, Z. Shaterzadeh-Yazdi, G. DiLabio, J. Mutus, J. Pitters, B. Sanders, R. Wolkow, "Dangling-bond charge qubit on a silicon surface", *New Journal of Physics*, vol. 12, no. 8, 083018, 2010.

[5] T. Kato, "On the adiabatic theorem of quantum mechanics", *Journal of the Physical Society of Japan,* vol. 5, no. 6, pp. 435 - 439, 1950.

[6] C. Lent, D. Tougaw, W. Porod, "Quantum cellular automata: the physics of computing with arrays of quantum dot molecules." *IEEE Workshop on Physics and Computation*, 1994.

[7] G. Mahan, *Many-Particle Physics,* Springer Science and Business Media New York, 2000.

[8] G. Mahler, and A. Volker, *Quantum networks, Dynamics of open nanostructures*, Springer-Verlag Berlin Heidelberg, 1998.

[9] U. Bockelmann, G. Bastard, "Phonon scattering and energy relaxation in two-, one-, and zero-dimensional electron gases", *Physical Review B,* vol. 42, no. 14, 8947, 1990.

[10] S. Barrett, G. Milburn, "Measuring the decoherence rate in a semiconductor charge qubit", *Physical Review B,* vol. 68, no. 15, 155307, 2003.

[11] S. Faleev, F. Lonard. "Theory of enhancement of thermoelectric properties of materials with nanoinclusions." arXiv preprint arXiv:0807.0260 (2008).

[12] C. Zener, "Non-adiabatic crossing of energy levels." *Proceedings of the Royal Society of London A: Mathematical, Physical and Engineering Sciences*, vol. 137, no. 833, pp. 696 - 702, 1932.

[13] J. Timler, C. Lent, "Power gain and dissipation in quantum-dot cellular automata", *Journal of Applied Physics*, vol. 91, no. 2, pp. 823 - 831, 2002.

[14] G. Santoro, et al. "Theory of quantum annealing of an Ising spin glass", *Science,* vol. 295, no. 5564 pp. 2427 - 2430, 2002.